論文

복합재 평판에 삽입된 광섬유 브래그 격자의 스펙트럼특성과 응력유도복굴절

이정률*, 김천곤**+, 홍창선**

Spectrum Characteristics and Stress Induced Birefringence of Fiber Bragg Grating Embedded into Composite Laminates

Jung-Ryul Lee*, Chun-Gon Kim**+, and Chang-Sun Hong**

ABSTRACT

Fiber Bragg grating(FBG) like other optical fiber sensors also has the merit of embedding capability. To increase their actual value related to embedding capability, this paper reported the reliability and signal characteristics of FBGs embedded in composite laminates. The microphotographs of embedded optical fibers visualized the embedding environments of stripped optical fibers and coated optical fibers. Based on these microphotographs and cure monitoring performed using FBGs, we could understand that the main cause breaking the unique Bragg condition of low-birefrigence FBG were residual stress after curing and reported the state of stress/strain of optical fiber quantitatively. The cure monitoring also showed the history of splitting peak of a stripped FBG along cure processing. In addition, we could obtain a transverse insensitive grating(TIG) with ease by recoating a stripped FBG. TIG has good advantage for real-time signal processing.

초 록

다른 광섬유 센서와 마찬가지로 광섬유 브래그 격자센서도 삽입가능의 장점을 가진다. 삽입가능과 관련된 실제적 가치를 높이기 위해서 본 논문에서는 복합재 평판에 삽입된 브래그 격자센서의 안전성과 스펙트럼특성이 연구되었다. 피복광섬유와 피복이 벗겨진 광섬유의 삽입 환경이 현미경 분석에 의해 수행되어졌고 이 현미경 사진들과 성형모니터링(cure monitoring)의 결과를 기초하여, 저복굴절(Lo-Bi) 광섬유에 새겨진 브래그 격자의 단일 브래그 조건을 붕괴하는 주원인이 성형 잔류응력임을 확인했고 이로 인해 광섬유가 겪게 되는 응력/변형률 상태를 정략적으로 보고하였다. 또한 성형모니터링은 브래그 공진파장이 어떻게 분리되어져 가는지 묘사하였고 횡응력 미감도 브래그 격자(TIG)가 재코팅 방법에 의해 쉽게 획득되어짐을 보였다. TIG는 실시간 신호 처리와 관련하여 중요한 장점으로 작용한다.

1. Introduction

Fiber Bragg gratings [FBGs] have been the subjects of intense development at many research centers around the world since the UV side writing technique was introduced in 1988[1]. One of the developments was the FBGs for axial strain sensor application[2] including temperature measurement [3]. FBG can be embedded in advanced composites and other materials to measure internal strain, temperature and other parameters. The first application of embedded FBG was an

* Mechanical and Materials Engineering Department, SMS division, Ecole Nationale Superieure des Mines de Saint Etienne, France.
** Department of Mechanical Engineering, Division of Aerospace Engineering, Korea Advanced Institute of Science and Technology(KAIST)
**+ Author to whom correspondence should addressed, Tel.: +82-42-869-3719, Fax: +82-42-869-3710, E-mail: cgkim@kaist.ac.kr

axial strain sensor inside an epoxy-fiber composite laminates [4].

There was another development of FBG. In 1995, it had been noticed that stress induced birefringence effects in low-birefringence (Lo-Bi) fibers can cause the unique Bragg condition to break down[5]. The transverse sensitive grating(TSG) has been also used as an simultaneous measurement sensor of longitudinal and transverse strain using low birefringence fiber[6] and high birefringence fiber[7]. In fact, these studies have been performed in order to detect errors due to transverse strains(for example residual strain, pressure, Poisson's ratio effect and so on) in the measurement of axial strain. In the latest studies, TSG was expanded into the high-pressure measurement sensor[8].

In this paper, spectrum characteristics of FBG embedded into composites were investigated. The chosen composite laminates have different characteristics in relation to orientation of reinforcement fiber, degree of residual stress and mechanical microbending. Finally, curing monitoring provides compressive understanding about the cause of birefringence of FBG embedded into composites. Finally, a recoating method to fabricate a TIG was introduced.

2. Theory

2.1 Structure of Single-Mode Fiber

An optical fiber is a dielectric waveguide that operates at optical frequencies. This fiber waveguide is normally cylindrical in form. Fig. 1 shows a schematic of a single-mode optical fiber.

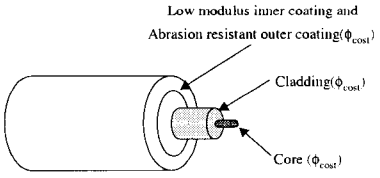

Fig. 1 Schematic of single mode optical fiber.

The core, having a refractive index n_{core} is surrounded by a solid dielectric cladding having a refractive index n_{clad}, that is less than ncore by 0.1~0.2%. The standard diameter of telecommunication fibers is 125μm. The coating increases diameter to about 250μm. Optical fiber has the dual protective acrylate coating, which is applied over the fiber cladding to cushion the fiber against microbending losses, provide abrasion resistance, and preserve the mechanical strength of the silica. Table 1 shows the properties and notations of the optical fiber used in this study. The optical fiber was made in Samsung Electronic co., Ltd.

Table 1 Specifications and strain-optic coefficients of optical fiber

Property	Value
Outer coating diameter	243.99m
Inter coating diameter	193.13m
Cladding diameter	124.58m
Core diameter	8.61m
Coating material	Acrylate
Poisson's Ratios(v_f)	0.16[9]
Effective core index(n_c)	1.4476
Photoelastic constant	P_{11}=0.113[10]
	P_{12}=0.252[10]
Young's modulus	70GPa

2.2 Birefringence of FBG

Ideal single-mode fibers preserve the state of polarization (SOP) of input light. However, in practice, optical fibers show birefringence by the following causes:

A1. Slightly elliptical optical fiber core.
A2. Intrinsic stress in an optical fiber.
A3. Transverse stress.
A4. Bending of an optical fiber.

A1 and A2 are classified the intrinsic birefringence and it presents in the fiber because of built-in anisotropies, either intentional or not. A3 and A4 are classified into induced birefringence. Once the fiber has been manufactured, it is almost impossible to induce any modification of its shape by external means because of the high Young's modulus of silica. But externally applied stresses and deformations can lead to induced birefringence through the photoelastic effect.

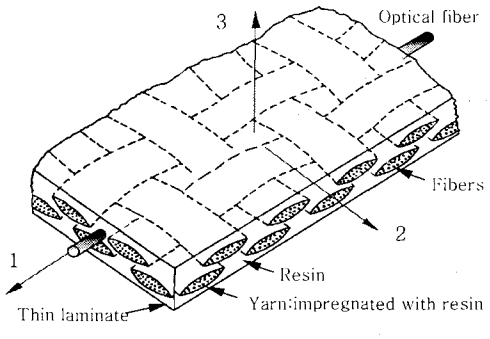

Fig. 2 Axis orientation of optical fiber embedded in a thin composite laminate.

If there is no intrinsic birefringence, the electronic field distribution can be approximated by the perfect degeneracy of two linear polarization(LP) modes. However, when the optical fiber shows birefringence, a 2-polarized excitation results in wave propagation with a different specific phase shift β compared to a 3-polarized excitation. The axis-orientation is shown in Fig. 2. The normalized birefringence is defined as:

$$B = \frac{\delta\beta}{\beta} \tag{1}$$

where $\beta=(\beta_2+\beta_3)/2=(\lambda_2+\lambda_3)/2$ is average propagation constant and $\delta\beta=\beta_3-\beta_2=\lambda_3-\lambda_2$ is birefringence.

In other words, the 2-polarized and 3-polarized LP modes don't have the same propagation constant any longer when the fiber exhibits some ellipticity of the core and/or some anisotropy in the refractive index distribution due to anisotropic stresses. If we jump to conclusion, the region stripped for the elaboration of a grating is exposed to anisotropic stress, for example, residual stress of composite in this experiment. Therefore, a reflected spectrum of FBG has two peaks and two axes of optically anisotropic medium are so-called a fast axis and a slow axis. This means that both shifts of two peaks should be considered to extract longitudinal strain because of perturbations of SOP. In practice, this acts a difficulty of dynamic strain measurement. The Bragg wavelength shifts in polarization axis of transverse sensitive grating(TSG) have complex forms such as following equations.

$$\frac{\Delta\lambda_2}{\lambda_{2.0}} = \varepsilon_1 - \frac{n_e^2}{2}\left[p_{11}\varepsilon_2 + p_{12}(\varepsilon_1+\varepsilon_3)\right] \tag{2}$$

$$\frac{\Delta\lambda_3}{\lambda_{3.0}} = \varepsilon_1 - \frac{n_e^2}{2}\left[p_{11}\varepsilon_3 + p_{12}(\varepsilon_1+\varepsilon_2)\right] \tag{3}$$

λ_2 and λ_3 indicates the resonance wavelengths of fast axis and slow axis, respectively. Index 0s means unperturbed states. When the stripped FBGs are embedded into composites, transverse residual stress after the vacuum bag mold process in an autoclave can induce such a birefringence. Inversely, these TSGs have been used to measure both longitudinal and transverse strain simultaneously in the limited mechanical applications [6-8]. For a FBG embedded into a composite laminate, we can assume two simplifications which are:

B1. to neglect the effect of transverse shear and
B2. to assume a state of plane stress
with respect to the 1-2 plane of Fig. 2.

The famous expression of the Hooke's law for a homogeneous isotropic material is the following.

$$\begin{pmatrix}\varepsilon_1\\ \varepsilon_2\\ \varepsilon_3\\ \varepsilon_4\\ \varepsilon_5\\ \varepsilon_6\end{pmatrix} = \begin{bmatrix} 1/E_f & -\nu_f/E_f & -\nu_f/E_f & 0 & 0 & 0\\ -\nu_f/E_f & 1/E_f & -\nu_f/E_f & 0 & 0 & 0\\ -\nu_f/E_f & -\nu_f/E_f & 1/E_f & 0 & 0 & 0\\ 0 & 0 & 0 & 1/G_f & 0 & 0\\ 0 & 0 & 0 & 0 & 1/G_f & 0\\ 0 & 0 & 0 & 0 & 0 & 1/G_f \end{bmatrix} \begin{pmatrix}\sigma_1\\ \sigma_2\\ \sigma_3\\ \sigma_4\\ \sigma_5\\ \sigma_6\end{pmatrix} \tag{4}$$

where E_f and G_f are the Young's modulus and shear modulus of the silica fiber. The hypotheses B1 and B2 mean that (σ_1 and σ_2 are nonzero and stress normal to the middle plane of the laminate and all shear stresses are zero, i.e. $\sigma_4=\sigma_5=\sigma_6=0$, the strain components in the principal directions of the optical fiber will result:

$$\varepsilon_1 = \frac{1}{E_f}(\sigma_1 - \nu_f\sigma_2)$$

$$\varepsilon_2 = \frac{1}{E_f}(\sigma_2 - \nu_f\sigma_1) \tag{4}$$

$$\varepsilon_3 = -\frac{\nu_f}{E_f}(\sigma_1+\sigma_2)$$

By substituting the strains in eq. (5) into the eq. (2) and (3), the Bragg wavelength shifts of the fast axis (λ_2) and slow axis (λ_3) can be represented as the followings.

$$\begin{pmatrix} \frac{\Delta\lambda_2}{\lambda_{2.0}} \\ \frac{\Delta\lambda_3}{\lambda_{3.0}} \end{pmatrix} = \begin{bmatrix} T_1 & T_2 \\ T_1 & T_3 \end{bmatrix} \begin{pmatrix} \sigma_1 \\ \sigma_2 \end{pmatrix}$$

$$T_1 = \frac{1}{E_f}\{1 - \frac{n_e^2}{2}[(1-\nu_f)p_{12} - \nu_f p_{11}]\}$$

$$T_2 = \frac{1}{E_f}\{-\nu_f - \frac{n_e^2}{2}[p_{11} - 2\nu_f p_{12}]\} \quad (6)$$

$$T_3 = \frac{1}{E_f}\{-\nu_f - \frac{n_e^2}{2}[(1-\nu_f)p_{12} - \nu_f p_{11}]\}$$

The inversion of the T matrix and data of Table 1 allows isolating the longitudinal and transverse stress by measuring the wavelength shifts of the two split peaks of a birefringent FBG.

$$\begin{pmatrix} \sigma_1 \\ \sigma_2 \end{pmatrix} = 70 \begin{bmatrix} 2.6939 & -1.4394 \\ 5.9172 & -5.9172 \end{bmatrix} \begin{pmatrix} \frac{\Delta\lambda_2}{\lambda_{2.0}} \\ \frac{\Delta\lambda_3}{\lambda_{3.0}} \end{pmatrix} GPa \quad (7)$$

Finally, we can realize that transverse stress is proportional to the distance between the two peaks alone because FBG unperturbed by birefringence has unique Bragg resonance wavelength ($\lambda_{B.0}=\lambda_{2.0}=\lambda_{3.0}$).

On the other side, in the case of transverse insensitive grating(TIG) the modes traveling along the fast axis and the slow axis are almost same. The exchange of power between them is thus very easy. After all, the refracted spectrum has one peak overlapped each other of which wavelength is Bragg resonance wavelength(λ_B). We next obtain very famous relation between longitudinal strain(ε_1) and Bragg wavelength shift such as:

$$\frac{\Delta\lambda_B}{\lambda_{B.0}} = \varepsilon_1\left[1 - \frac{n_e^2}{2}\{p_{12} - \nu_f(p_{11} + p_{12})\}\right] \quad (8)$$

In practice, we could obtain TIGs by acrylate recoating method.

3. Experiments and Results

3.1 Signal Characteristics of FBGs and Embedding Reliability

To investigate the spectrum of embedded FBG changed by the state of stress in the circumference of an optical fiber after curing and the embedding reliability of optical fiber, optical fibers were embedded parallel($[0_5/\{0\}/0_5]$: Case Ⅰ) and perpendicular($[90_5/\{0\}/90_5]$: Case Ⅱ) to unidirectional reinforcement fiber of Graphite/Epoxy laminates. We next embedded optical fibers to plain-weave Glass/Epoxy fabric composites. In the case of unidirectional reinforced composites, the thickness of a prepreg was 0.125 mm. For plain-weave fabric composites, the embedding environments of optical fibers were quite different from the unidirectional cases because of undulating yarns. One yarn of CaseⅢ ([4plies/{OF}/4plies]) is composed of 200 E-glass fibers and the thickness of a prepreg is 0.18 mm. One yarn of CaseⅣ ([3plies/{OF}/3plies]) includes 600 E-glass fibers and the thickness of a prepreg was 0.22 mm.(see Fig. 3(a), Fig. 4(a), and Fig. 4(c)) Each diameter of a bare optical fiber (OF), a graphite fiber and a glass fiber was 125 μm, 7 μm and 10 μm, respectively. The geometries of specimens were 250mm×100mm×1.25mm in Case Ⅰ and Case Ⅱ, 250mm×100mm×1.44 mm in CaseⅢ, and 250mm×100mm×1.32mm in CaseⅣ. Fig. 4(b) represents the positions of grating and the ways of ingress of specimens.

For the cure residual stress, the two main components[11] that contribute to this stress are:

C1. The volumetric shrinkage of the resin during cure
C2. The mismatch in the coefficient of thermal expansion (CTE) of the matrix and the reinforcement.

Therefore, Case Ⅰ and Case Ⅱ with only unidirectional *prepregs were chosen to distinguish the volumetric shrinkage* effects of the resin. CaseⅢ with plain-weave fabric prepregs was chosen as the case with serious residual stress. In general, the plain-weave fabric laminates have even greater residual stress after cure processing because of the higher volumetric shrinkage by reason of smaller fiber volume fraction and the mismatch in the CTE between the matrix and the perpendicularly crossed fibers.

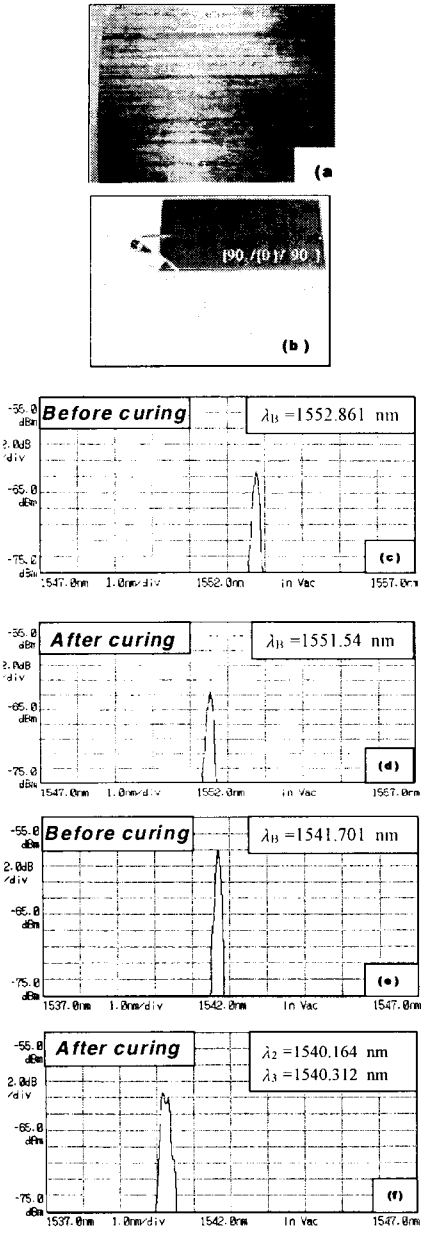

Fig. 3 Reflected spectra of Case I and Case II: (a) Unidir ectional prepreg of Case I and Case II, (b) Specimen of Case II, (c) Case I before curing, (d) Case I after curing, (e) Case II before curing, (f) Case II after curing (by LED- OSA system).

As for embedding reliability, CaseIV was selected as the case with much higher mechanical microbending than Case I, Case II and CaseIII. Fig. 5(a)-(c) shows the degree of microbending of Case I, Case II and CaseIII.

As shown in Fig. 3(f) and Fig. 4(e), transverse stress after curing caused birefringence of optical fiber contrary to Case I of Fig. 3(d). In other words, the birefringence effects caused unique Bragg conditions to break down slightly in Case II ($B=9.61\times10^{-5}$), and even produced two very distinct resonance wavelengths in the CaseIII($B=2.46\times10^{-4}$). Considering eq. (7), we could understand that the transverse stress of CaseIII was much higher than that of Case II. This distortion of unique Bragg condition may cause some ambiguity to isolate longitudinal strain. Above all, fast signal processing to measure dynamic strain becomes difficult.

To provide understandings about embedding environments of optical fiber, we inspected microscopically the polishing cross sections(see Fig. 5(d)-5(h)). These microphotographs were taken with an optical microscope(OLYMPUS) at 100x or 200x magnification. These microphotographs helped us to understand the various characteristics of the embedded optical fibers. The embedding environment of Case I shown in Fig. 5(d) kept unique Bragg condition in spite of the shrinkage of resin. The exchange of power between the two modes was very easy because small transverse residual stress induced low birefringence. Therefore the reflected spectrum has one peak overlapped each other. In general, Case II of which optical fiber embedded perpendicular to reinforcement fibers, should have smaller transverse residual stress because the degree of reinforcement fiber shrinkage is much smaller than that of the resin shrinkage. However the spectrum of Case II had two peaks. The cause about this unexpected phenomenon could be found out in Fig. 5(e). The bare optical fiber embedded perpendicular to the reinforcement fibers had two resin rich regions in its both sides. These resin rich regions induced additional transverse stress. In other words, the cause of the birefringence in Case II was not proper transverse residual stress of the composite laminate but resin rich regions generated by embedding the 125μm optical fiber. Fig. 5(f) shows the cross section in the surrounding of the bare optical fiber in CaseIII. This case produced two very distinct peaks induced by transverse residual stress(see Fig. 4(e)). As shown in Fig. 5(g), the dual acrylate coating of optical fiber became an elliptic shape because of temperature and pressure during the cure processing. It made small spaces between coating and optical fiber. The dual protective acrylate coating and the spaces will act on the fiber cladding as a cushion against

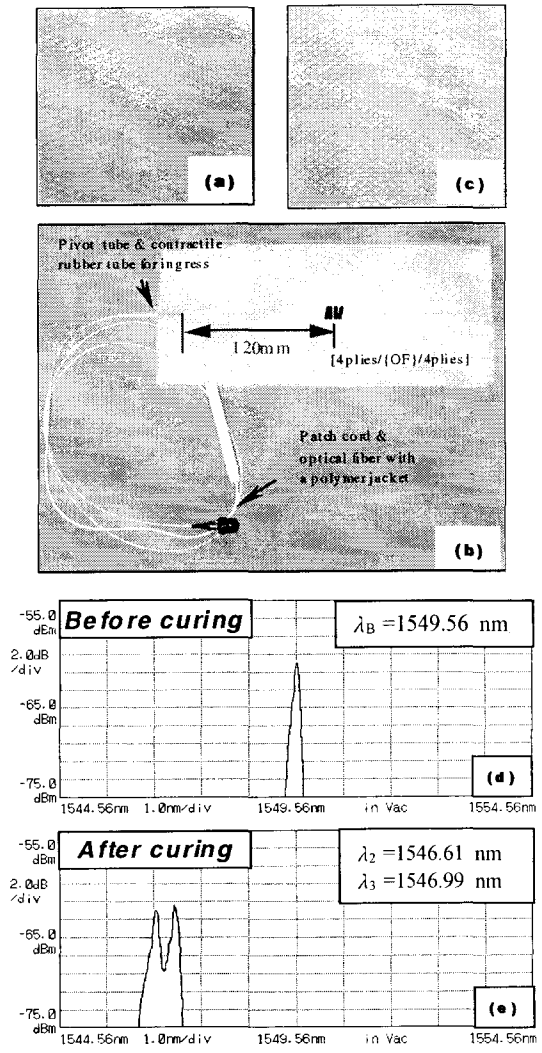

Fig. 4. Reflected spectra of CaseIII and Prepreg of Case IV:(a) Prepreg of CaseIII, (b) Specimen of Case III, (c) Pre preg of CaseIV with bigger yarns, (d) Spectrum of CaseIII before curing, (e) Spectrum of CaseIII after curing.

transverse stress. Similarly, FBG recoated by the same material(acrylate) was also protected from transverse residual stress lest reflected FBG spectra should be split in two peaks (see Fig. 9). Judging from the embedding environment of optical fiber in Fig. 5(h), a recoated FBG embedded in Case IV may be also safe from transverse residual stress.

In the second place, microbendings cause light losses and backscatters optically and may lead to stress fractures of optical fiber mechanically. As for peak in spectrum of FBG, intensity loss is not important until fibers are separated by fracture. Therefore, mechanical microbending effects are more important than optical microbending effects relatively. As shown in Fig. 5(a), 5(b), and 5(c), very thin Teflon films were embedded in Case II, III and Case IV in order to observe the degree of mechanical microbending. Contrary to Fig. 5(i) and 5(j), we could see the stress fractures of bare optical fiber in Fig. 5(k). The optical fiber failed mechanically because of serious undulation of yarns. In Fig. 5(l) of Case III and Fig. 5(m) of CaseIV, however, the coatings protected bare optical fibers against microbending failures. In addition, four microphotographs(Fig. 5(g), (h), (l) and (m)) of the cases with coatings showed that although the cure temperature(130℃) was close to the breakdown temperature of the acrylate coating(150℃), the coatings were not melted and survived during the cure processing.

Consequently, the birefringence of embedded FBGs depended on the orientation of optical fiber relative to the reinforcement fibers, the degree of transverse residual stress. The recoating of stripped FBG was also very important for the purpose of relieving birefringence phenomenon optically and microbending effects mechanically.

3.2 Cure Monitoring to Study Transverse Stress Induced Birefringence

The cure monitoring was performed in order to observe the history of FBG spectrum and the change in wavelength during the cure processing. The specimen has the same geometry and material as Fig. 4(b). The gratings were a stripped FBG and a recoated FBG. The coating of optical fiber was stripped to build a grating in the optical fiber using a KrF excimer laser and a phase mask. The stripped FBG was recoated by VYT-200-C using the same material (acrylate). WSFL[12]-DPO FBG sensor system with higher power(2.2mW) was used because of the causes of serious microbending loss inside an autoclave and at its door part. The set up for this experiment is shown in Fig. 6. Fig. 7(b) shows the shifts in wavelength obtained by embedded FBGs during the typical cure cycle shown in Fig. 7(a). It is similar to the temperature curve of specimens by a thermocouple because of the linear dependence of the Bragg wavelength with temperature. Birefringence onset time was 182 min in the experimental time. Before second holding step, the spectra

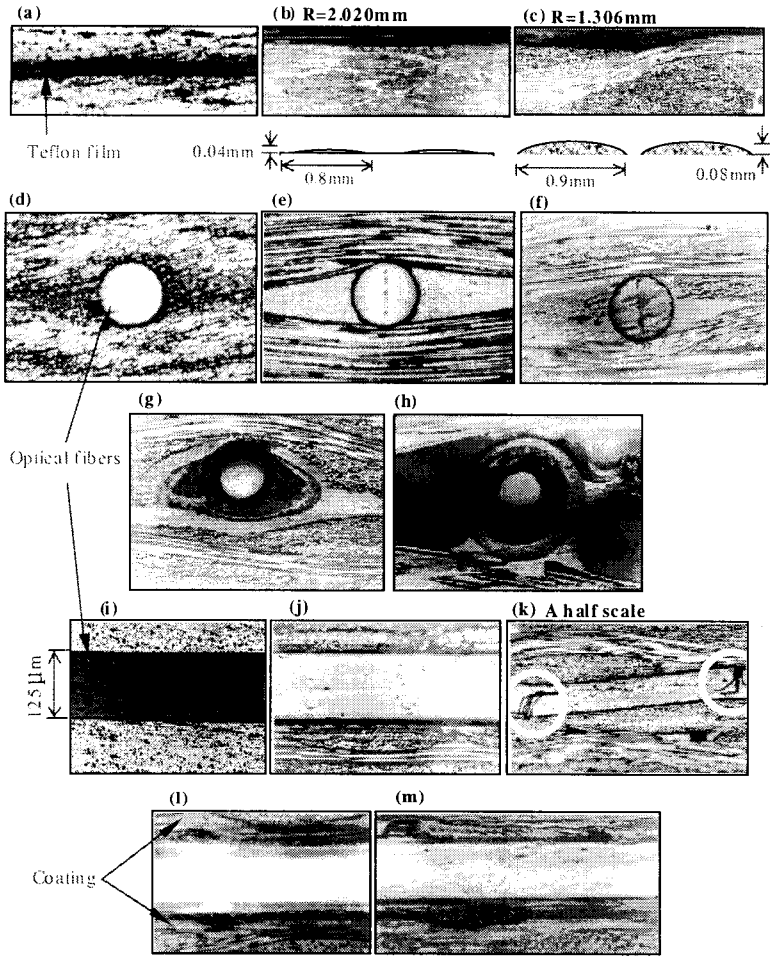

Fig. 5 Embedding environments of bare optical fibers and coated optical fibers: (a), (b) and (c) Embedding environments of Case Ⅱ, Ⅲ and Ⅳ, (d), (e) and (f) Cross sections of bare optical fibers embedded in Case Ⅰ, Case Ⅱ, Case Ⅲ, (g) and (h) Cross sections of optical fibers with dual acrylate coatings in CaseⅢ and Case Ⅳ, (i), (j) and (k) Side sections of bare optical fiber in Case Ⅱ, CaseⅢ and Case Ⅳ, (l) and (m) Side sections of optical fibers with dual acrylate coatings in Case Ⅲ and Case Ⅳ.

of the stripped FBG were not changed in spite of the application of cure pressure. This means that curing pressure (σ_3) is not enough to induce the birefringence phenomenon. The stripped FBG also remained one peak during the 2nd holding step. We couldunderstand that the gradual progress in the shrinkage of resin during the 2nd holding was still not enough to induce birefringence. After beginning the cooling step and removing the cure pressure(6 atm.=607.95 KPa), the rapid increase in the residual stress, which was promoted by the mismatch in the CTE between the resin and reinforcement fibers, induced an additional peak at the onset time of birefringence and the distance between two peaks increased more and more until room temperature(see Fig. 7(b) and 8(a)). The last graph in Fig. 8(a) is the spectrum of the birefringent FBG after taking the specimen out of an autoclave and controlling polarization. However any additional peak did not appear in the spectra of the recoated FBG shown in Fig. 8(b). This means that the recoating protected the FBG from the transverse residual stress since the cooling step and the use of recoating has made possible easy

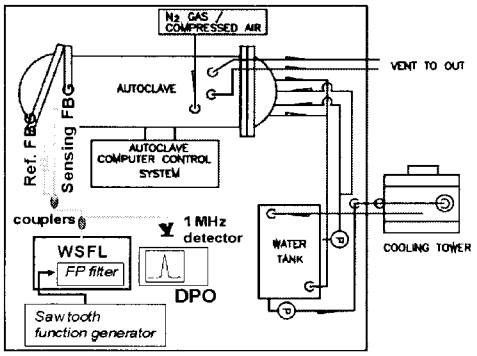

Fig. 6 Set up for cure monitoring.

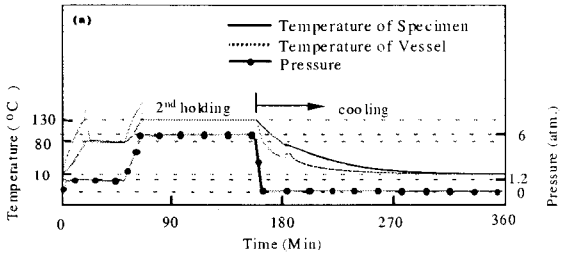

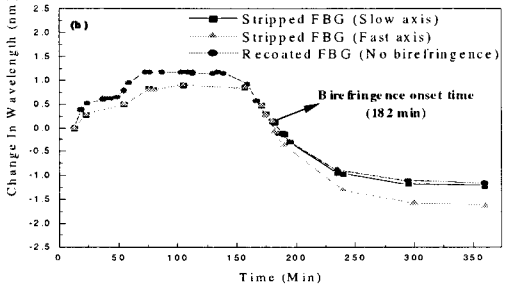

Fig. 7 Changes in wavelength of a stripped FBG and a recoated FBG: (a) Cure cycle, (b) Cure monitoring.

fabrication of TIG. The normalized birefringence (B), the longitudinal and the transverse strain of the stripped FBG were 2.56×10^{-4}, -1436 με and -1267 με. Because σ_3 inducing minus birefringence against σ_2 existed in spite of small value, the transverse strain showed smaller contraction than the longitudinal strain. The longitudinal strain of the recoated FBG (-943 με) showed smaller contraction than that of the stripped FBG (-1436 με). For the recoated FBG, the good

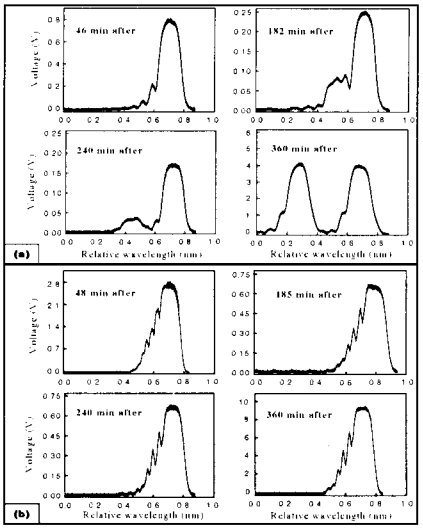

Fig. 8 Changes in spectrum: (a)Stripped, (b)Recoated FBG.

strain transfer between the composite material and the optical fiber might be not guaranteed because of the acrylate recoating.

4. Conclusion

The reliability and spectrum characteristics of FBGs embedded in composites laminates were studied in this paper. The microphotographs of embedded optical fibers visualized the embedding environments of stripped optical fibers and coated optical fibers. Based on these microphotographs and cure monitoring performed using FBGs, we could understand that the main cause breaking the unique Bragg condition of low-birefrigence FBG were residual stress after curing and reported the state of stress/strain of optical fiber quantitatively. The cure monitoring also showed the history of splitting peak of a stripped FBG along cure processing. In addition, we could obtain a TIG with ease by recoating a stripped FBG.

Acknowledgement

The authors would like to thank the Ministry of Science

and Technology, Korea and Korea Science and Engineering Foundation for the financial support for Korea-France Joint Projects.

References

1) G. Meltz, W. W. Morey, W. H. Glenn, and J. D. Farina, "In-fiber Bragg-grating sensors," *OFS'88*, New Orleans, Louisiana, 1988, p. 163.
2) G. Meltz, W. H. Glenn, E. Snitzer, "Distributed spatially resolving optical fiber strain gauge," U.S. Patent No. 4,761,073, August 2, 1998.
3) W. W. Morey, et al., "Bragg-grating temperature and strain sensors," *OFS'89*, Paris, 1989, p. 526.
4) J. R. Dunphy, G. Meltz, F. P. Lamm, W. W. Morey, "Multi-function, distributed optical fiber sensor for composite cure and response monitoring," *SPIE1370*, Bellingham, 1990, pp. 116-118.
5) J. R. Dunphy, et al., United States Patent 5,399,854, March 21, 1995.
6) R. B. Wagreich, Atia, W. A., Singh, H., Sirkis, J. S. "Effects of diametric load on fibre Bragg gratings fabricated in low birefringence fibre," *Electronics Letter*, Vol. 32, No. 13, 1996, pp. 1223-1234.
7) C. M. Lawrence, D. V. Nelson, E. Udd, T. Bennett, "Measurement of transverse strains with fiber Bragg gratings," *Experimental Mechanics*, Vol. 39, No. 3, 1999, pp. 202-209.
8) Robert, J. S., Tsutomu, Y., "High pressure and temperature sensing for the oil Industry using fiber Bragg gragtings written onto side hole single mode fiber," *OFS-13*, Kyongju, 1999, pp. 42-45.
9) N. Lagako and J. Bucaro, "Pressure desensitization of optical fibers," *Applied Optics*, Vol. 20, 1981, pp. 2716-2720.
10) A. Bertholds and R. Dandlker, "Determination of the individual strain-optic coefficients in single-mode optical fibers," *Journal of lightwave Technology*, Vol. 6, No. 1, 1988, pp. 17-20.
11) L. K. Jain, B. G. Lutton, Y. W. Mai, R. P, "Stress and Deformations Induced during Manufacturing. Part II: A Study of the Spring-In Phenomenon," *Journal of Composite Materials*, Vol. 31, No. 7, 1997, pp. 696-719.
12) S. H. Yun, D. J. Richardson, and B. Y. Kim, "Interrogation of Fiber Grating Sensor Arrays with a Wavelength-Swept Fiber Laser," *Optics Letters*, Vol. 23, No. 11, 1998, pp. 843-845.